**Climate
of the Past
Discussions**

Continuous and self-consistent CO$_2$ and climate records over the past 20 Myrs

R. S. W. van de Wal[1], B. de Boer[1], L. Lourens[2], P. Köhler[3], and R. Bintanja[4]

[1]Institute for Marine and Atmospheric research Utrecht, Utrecht University, Princetonplein 5, 3584 CC Utrecht, The Netherlands
[2]Department of Earth Sciences, Faculty of Geosciences, Utrecht University, Budapestlaan 4, 3584 CD Utrecht, The Netherlands
[3]Alfred Wegener Institute for Polar and Marine Research, P.O. Box 120161, 27515 Bremerhaven, Germany
[4]Royal Netherlands Meteorological Institute (KNMI), Wilhelminalaan 10, 3732 GK De Bilt, The Netherlands

Correspondence to: R. S. W. van de Wal (r.s.w.vandewal@uu.nl)

Abstract

The gradual cooling of the climate during the Cenozoic has generally been attributed to a decrease in CO_2 concentration in the atmosphere. The lack of transient climate models and in particular the lack of high-resolution proxy records of CO_2, beyond the ice-core record prohibit however a full understanding of the inception of the Northern Hemisphere glaciation, as well as the mid-Pleistocene transition. Here we elaborate on an inverse modeling technique to reconstruct a continuous high-resolution CO_2 record over the past 20 Ma, by decomposing the global deep-sea benthic $\delta^{18}O$ record into a mutually consistent temperature and sea-level record, using a set of 1-D models of the major Northern and Southern Hemisphere ice sheets. We subsequently compared the modeled temperature record to ice core and proxy-derived CO_2 data to reconstruct a continuous CO_2 record over the past 20 Myrs. Results show a gradual decline from 450 ppmv around 15 Myrs ago to 280 ppmv for pre-industrial conditions, coinciding with a gradual cooling of the Northern Hemisphere land temperatures by approximately 12 K, whereas there is no long-term sea-level variation caused by ice-volume changes between 13 to 3 Myrs ago. We find no evidence for a change in climate sensitivity other than the expected decrease following from saturation of the absorption bands for CO_2. The reconstructed CO_2 record shows that the Northern Hemisphere glaciation starts once the average CO_2 concentration drops below 265 ppmv after a period of strong decrease in CO_2. Finally it might be noted that we observe only a small long-term change (23 ppmv) for CO_2 during the mid-Pleistocene transition.

1 Introduction

The gradual climate cooling reconstructed for the past 20 Myrs has generally been attributed to a change in CO_2 concentration in the atmosphere (Zachos et al., 2008; Ruddiman, 2003), although the amount of CO_2 decrease and the amplitude of subsequent cooling are discussed widely (Jansen et al., 2007). Since data and modeling

studies covering this time period are poorly integrated, our understanding of the inception of ice ages in the Northern Hemisphere (NH) (Raymo, 1994), as well as the mechanisms causing the transition from 41 000-year to 100 000-year dominated climate cycles (Tziperman and Gildor, 2003; Clark et al., 2006; Huybers, 2007; Bintanja

5 and Van de Wal, 2008), that occurred without apparent changes in the insolation forcing (Hays et al., 1976; Imbrie and Imbrie, 1980) is still incomplete. Current difficulties in assessing the role of CO_2 on the long time scales are the lack of reliable CO_2 data from the pre ice-core record (Ruddiman, 2010), and the limited data of sea level (Miller et al., 2005; Müller et al., 2008) and temperature (De Boer et al., 2010). Our cur-

10 rent knowledge on long-term climate variability builds on the Milankovitch theory of solar-insolation variability (Milankovitch, 1941), including scenarios that rely on highly parameterized non-linear response mechanisms to the insolation forcing. Recent developments in the interpretation of marine $\delta^{18}O$ records and new CO_2 proxies allow us to reassess this understanding and to present a global overview of temperature, sea

15 level and CO_2 changes over time.

   We build on a model set-up that aims to integrate climate variables. In the early stages it was used by Bintanja et al. (2005a) to calculate ice age temperatures with sea level as external forcing. Rather than forcing a model with an independent temperature proxy and calculating ice-volume change, we forced by then the ice-sheet model

20 with sea level, and reconstructed the temperature necessary to match the sea-level observations. This model includes an inverse routine, which related a perturbation in NH atmospheric temperature relative to present day to the difference between modeled and observed sea level. Modeled ice volume was compared to observed sea level, and temperature was adjusted such that modeled ice volume matched the observa-

25 tions. This constraint ensured that sea level and temperature are mutually consistent. In addition it allowed a quantification of model errors, and errors arising from the uncertainty in the sea-level observations or reconstructions. Results have been compared favorably with data by Rohling et al. (2009) and Lambeck and Chapell (2001) for sea level, and Lear (2000) for temperature. Nevertheless an obvious limitation of this work

Title Page

Abstract | Introduction

Conclusions | References

Tables | Figures

◄◄ | ►►

◄ | ►

Back | Close

Full Screen / Esc

Printer-friendly Version

Interactive Discussion

was that global sea-level observations are limited to the last 0.5 Myrs. Therefore later studies used the same inverse approach, but used the marine benthic δ^{18}O record as forcing (e.g. Bintanja et al., 2005b). This was achieved by taking advantage of mass conservation of δ^{18}O on the global scale. First, It was applied to calculate temper-
5   ature and sea level over the past million years (Bintanja et al., 2005b), and later to explore the mechanisms of the Mid-Pleistocene Transition (Bintanja and Van de Wal, 2008), both focusing on the climate in the Northern Hemisphere, as only the Eurasian and North American ice sheet complexes were modeled explicitly. In order to use the benthic δ^{18}O record as forcing, a simple deep-water temperature model was used to
10   separate the marine benthic record changes in deep-water temperature changes and ice-volume changes. The last step in the model sequence until now is the explicit inclusion of ice sheets in the Southern Hemisphere (SH) to allow the study of the entire Cenozoic (De Boer et al., 2010).

In this paper we will use their Cenozoic reconstruction in terms of temperature and
15   sea level to compare existing proxies for CO_2 to our reconstructed temperature beyond the ice-core record. The reconstructed temperature is based on a stacked deep-sea record (Zachos et al., 2008), and models of the five major ice sheets in (North America, Eurasia, Greenland, East- and West-Antarctica, further abbreviated to NAIS, EAIS, GrIS, EAIS, WAIS). This temperature, which is self-consistent with the deep-sea
20   record, is then compared to the ice-core CO_2 record (Petit et al., 1999; Siegenthaler et al., 2005; Lüthi et al., 2008) over the past 800 000 years. This comparison allows us to select existing CO_2 proxies, which are consistent with reconstructed temperature, and hence self-consistent with the deep-sea record. These selected CO_2 records are then used to determine a regression coefficient between temperature and CO_2,
25   which is used to reconstruct a global mutually self-consistent and continuous overview of temperature, sea level and CO_2 over the past 20 Myrs.

◄◄ | ►►

◄ | ►

Back | Close

Full Screen / Esc

Printer-friendly Version

Interactive Discussion

2 Inverse δ^{18}O modeling approach

The inverse modeling approach enables the deep-sea benthic δ^{18}O record to be decomposed in a temperature and ice-volume component by simulating changes in NH temperatures and five ice sheets in Northern and Southern Hemisphere, representative
5 for glaciations on Earth (Bintanja et al., 2005b; de Boer et al., 2010). Key processes in the ice-sheet model are a variable isotopic sensitivity and isotopic lapse rate, the mass balance height feedback, the mass balance albedo feedback and the adjustment of the underlying bedrock. The methodology is a continuation of previous work performed with 3-D ice-sheet models over the Plio-Pleistocene (Bintanja et al., 2005b; Bintanja
10 and Van de Wal, 2008).

The key difference with the old model set up and the present work by de Boer et al. (2010) is the inclusion of ice in the SH, allowing a longer time span to be covered, since for warmer conditions ice-volume changes are dominated by changes in the Southern Hemisphere. This is done at the expense of the complexity of the ice-
15 sheet models used, to keep computing time manageable. In order to run over 35 Myrs we now explicitly simulate five 1-D ice sheets, rather than the two 3-D ice-sheet models used by Bintanja et al. (2005b) and Bintanja and Van de Wal (2008). The five 1-D ice-sheet models simulate ice flow over a cone shaped continent (De Boer et al., 2010). They represent glaciation in Eurasia, North America, Greenland and East and West
20 Antarctica, where each has a different geometry, mass balance forcing and isotopic content.

The key parameter to be simulated is still the change in the NH temperature (ΔT_{NH}), which determines the growth of ice, and changes in the deep-water temperature and the SH temperatures. To obtain atmospheric temperatures a simple parameterization
25 is used to relate deep-water temperature to atmospheric temperature (Bintanja et al., 2005b). In addition we include a simple parameterization of the temperature difference between the Northern and the Southern Hemisphere, which is used to calculate growth and decay of ice in the Southern Hemisphere. This parameterization contributes to the

uncertainty of the model as will be explained later. The conceptual approach used here was developed for orbital time scales. Thus the antiphase dynamics of temperature in northern and southern high latitudes as observed for the bipolar seesaw (e.g. Barker et al., 2009) is not embedded here, neither are Dansgaard/Oeschger events resolved.

5   In the ice-sheet model, isotopic content and ice volume are calculated with a time step of 1 month and are implemented every 100 years in the ocean isotope module. Every 100 years, the modeled benthic isotope is evaluated and forwarded to calculate the temperature anomaly for the next time step (Bintanja et al., 2005b).

As forcing we use the stacked benthic δ^{18}O record of Zachos et al. (2008), which is
10 smoothed and interpolated to obtain a continuous record with a resolution of 100 years. This implies that the time scale of the reconstruction is implicitly determined by the benthic record. The methodology ensures that the phasing between temperature and sea level is consistent with respect to the benthic δ^{18}O data. Further details and a more thorough model description are presented by de Boer et al. (2010).

15 **3   Results in terms of sea level and temperature variability**

Our model-based deconvolution shows a long-term decrease in T_{NH} by 12 K since the Miocene with superimposed orbitally forced changes, Fig. 1. Eustatic sea level, more strictly sea level from ice-volume changes only, gradually falls, but is roughly constant from 13 Ma (+15 m) to 3 Ma (+5 m) as the ice sheets in the SH are full grown and
20 major ice sheets in the NH are not yet developed (Fig. 1c). Moreover, the deviation of the sea-level changes from the 400 kyr running mean revealed only low amplitude sea-level changes of 10 m during this time period, whereas it fluctuated up to +20 m prior to 13 Ma and up to 66 m after 3 Ma. Maximum sea level high-stand of +55 m occurred around 15 Ma, probably caused by a reduced East Antarctic ice Sheet (De Boer et al.,
25 2010).

Figure 2 shows that there is not a unique solution for sea level given a certain temperature. This results from the different time scales in the coupled system of ice sheets,

changing deep-water temperatures, surface temperatures, bedrock adjustment, and forcing and feedbacks of the mass balance height and albedo-temperature feedback. Obviously, sea level rises on average with temperature as illustrated by the thick lines in Fig. 2a. On average the sea-level change is 6 m per Kelvin temperature change.

5   Close to present-day temperatures, i.e. $\Delta T_{NH} > -2$ K to $\Delta T_{NH} < +10$ K, only the Greenland and West Antarctic ice sheets change in size, resulting in only minor sea-level fluctuations (Fig. 2b), which are approximately 5 times lower compared to warm or cold conditions, expressed per Kelvin temperature change. During warmer ($\Delta T_{NH} > +10$ K) and colder climates ($\Delta T_{NH} < -2$ K), sea-level changes were stronger due to variations

10 in the size of the large North American, Eurasia and East Antarctic ice sheets. For colder climates the large NH ice sheets are vulnerable to environmental changes, for warmer climates Antarctica is sensitive to temperature changes with an average sensitivity (Δ Sealevel/ΔT_{NH}), which is approximately similar for warm and cold climates as indicated by the thick line in Fig. 2a. In addition Fig. 2b shows the volume change

15 for the individual ice sheets as a function of temperature leading by summation to the complex pattern in Fig. 2a. Also on the level of an individual ice sheet, transient effects impede a simple and unique solution between temperature and sea level, which implies that inverting climate information from sea-level records has to be considered with care.

20   In contrast to the sea-level record, temperature shows a more gradually decline from the Miocene maximum around 15 Myrs ago to the start of the major glaciation in the Northern Hemisphere around 3 Ma. The gradual increase in the benthic δ^{18}O record leads to a long-term cooling of the climate between 13 and 3 Ma. The amplitude of temperature and sea-level variability both increase once the major ice sheets develop

25 in the Northern Hemisphere around 3 Myrs ago.

    Many tests have been performed with the model to assess the uncertainties in the input and model parameters on sea level and temperature results. The most important tests allow us to estimate the uncertainty range displayed in Fig. 1. For the δ^{18}O input we defined an uncertainty of 0.16‰, which is derived from the root mean squared

difference between the smoothed marine record and the actual data points. The key model parameters contributing to the uncertainty are (1) the deep-water to surface-air temperature coefficient (range 0.15 to 0.25), (2) the temperature difference between the NH temperatures and the temperatures around Antarctica (range: 6–14 K for EAIS, range: 2–10 K for WAIS), and (3) the isotopic content of the ice sheets (range from −43, −32, −28 to −55, −42, −36‰ respectively for EAIS, WAIS, GrIS), see De Boer et al. (2010) for details. For the three model parameters, maximum and minimum values are used to test the effect on modeled temperature and sea level. The resulting standard deviation varies over time, but is on average 1.9 K for temperature and 6.2 m for sea level over the past 20 Myrs.

In order to interpret the results one has to bear in mind that the reconstructed temperatures are strictly only valid in the continental areas where ice sheets develop in the NH (ΔT_{NH}), being mid to sub polar (NH) latitudes (Bintanja et al., 2005a), implying that they are therefore not necessarily representative for the entire globe (ΔT_g).

4   Reconstruction of CO$_2$

Intriguing is the question how these changes in temperature and sea level are related to changes in CO$_2$. In order to get a consistent CO$_2$ record, we investigated the relation between temperature and proxy CO$_2$ records based on B/Ca ratio (Tripati et al., 2009), stomata (Kürschner et al., 2008), δ^{11}B (Pearson and Palmer, 2000; Hönisch et al., 2009), alkenones (Pagani et al., 2005, 2009), a combination of alkenones and δ^{11}B (Seki et al., 2010), and ice cores (Petit et al., 1999; Siegenthaler et al., 2005; Lüthi et al., 2008), all shown in Fig. 3. All data points are representative for different discrete time intervals, with obviously a bias towards the more modern data points and each having its advantages and drawbacks. For example, the boron isotope derived estimates of the CO$_2$ concentration are based on the fact that higher atmospheric concentrations lead to more dissolved CO$_2$ in the surface ocean, which cause a reduction in the pH of the ocean. As the pH can be derived from measurements of the δ^{11}B of

calcium carbonate (Pearson and Palmer, 2000), CO_2 can be calculated provided that another parameter of the marine carbonate system (e.g. alkalinity) is known (Zeebe and Wolf-Gladrow, 2001). The method is expensive, time consuming, and only well-preserved foraminiferal specimen are suitable for the analysis, resulting in up to now only low-resolution records. Ice cores provide the most robust and high-resolution CO_2 archive as they directly preserve the atmospheric concentrations, but only for the past 800 000 years (Lüthi et al., 2008). Here, we accept all data as they are published without any further correction. The general picture is that the scatter in the different approaches is large, but there is a tendency for higher CO_2 values in the early Cenozoic (Ruddiman, 2003; Zachos et al., 2008), with ambiguous results for the last 20 Myrs. Moreover none of the proxies has a continuous record for the entire Cenozoic (Fig. 3). For this reason there is a need to compile all available records in a consistent manner. The decomposition of the marine benthic $\delta^{18}O$ record offers a framework to do so.

We use the modeled temperature as a tool to select mutually consistent CO_2 records by assuming that there is a relation between CO_2 and temperature, which is comparable to the relation found in ice cores. Figure 4 shows the various CO_2 estimates against our reconstructed NH temperatures. A possible explanation for the fact that $\delta^{11}B_h$ ($\delta^{11}B$ from Hönisch et al., 2009) is consistent with CO_2 from the ice cores and $\delta^{11}B_p$ ($\delta^{11}B$ from Pearson and Palmer, 2000) shows a different slope, is the different methodology followed, where Hönisch et al. (2009) only used a single species, Pearson and Palmer (2000) used multispecies. The comparison in Fig. 4 reveals that the CO_2 estimates derived from the ice cores, B/Ca, $\delta^{11}B_h$ and the combination of alkenones and $\delta^{11}B_s$ ($\delta^{11}B$ from Seki et al., 2010) are mutually consistent, because they have a similar slope, whereas the $\delta^{11}B_p$, alkenones and stomata-derived CO_2 estimates do not show a consistency with the ice-core record.

We therefore only selected the consistent records to derive an empirical relationship between temperature and CO_2. This relation between temperature and CO_2 is used to calculate CO_2 from temperature in order to generate a continuous CO_2 proxy record, which is consistent with the benthic $\delta^{18}O$ record and continuous in time. The

Continuous and self-consistent CO_2 and climate records over the past 20 Myrs

R. S. W. van de Wal et al.

Title Page

Abstract	Introduction
Conclusions	References
Tables	Figures

◄◄ | ►►

◄ | ►

Back | Close

Full Screen / Esc

Printer-friendly Version

Interactive Discussion

application of the correlation between CO$_2$ and temperature implies that the regression needs to cover the temperature range as shown in Fig. 1 without having too much bias to the data rich cold climate state. For this reason, we binned the CO$_2$ observations in intervals of 1 K NH temperature change, for which results are shown in Fig. 5. The temperature records are running averages over 2000 years, in order to prevent outliers due to a mismatch in dating of the CO$_2$ proxy and the benthic record. Furthermore, several tests have been performed to weigh the different accepted CO$_2$ proxies, by uncertainty in modeled temperature and measured CO$_2$. In addition, we tested the effect of the binning size and averaging period, which contribute to the uncertainty in the reconstructed CO$_2$. Eventually we estimated based on all these tests an uncertainty of 10% in the slope between $\ln(CO_2/CO_{2,\mathrm{ref})}$ and ΔT_{NH} around a central value of 39 K. A log-linear regression between ΔT_{NH} and CO$_2$ is used because of the saturation of the absorption bands for CO$_2$ (Myhre et al., 1998), see also next section.

As a result of the 10% uncertainty in C, the CO$_2$ as presented in Fig. 1 has an uncertainty of 20 ppmv for cold climates and up to 45 ppmv for warm climates.

Over the past 800 kyr the reconstructed CO$_2$ record is in good agreement with the ice-core record, (Fig. 6c), which is, however, input to the reconstruction and therefore not an independent result. On the other hand it is noteworthy to mention because the ice-core CO$_2$ data are significantly lower during the earliest two glacial maxima recorded in the ice between 0.6 and 0.8 Ma. Over the mid-Pleistocene transition (defined here from 1.5 to 0.5 Myrs), our results indicate a gradual decline of about 23 ppmv since the average level near 1.5 Ma, and at the same time an increase in the amplitude. Carbon-cycle simulation results over the last 2 Myr across the Mid-Pleistocene Transition (Köhler and Bintanja, 2008) support the change in amplitude, but suggest stable glacial CO$_2$ values and reduced interglacial CO$_2$. It is also unclear why the combined δ^{11}B and Alkenone record is higher than our reconstruction for the last 1.5 Myrs.

More remarkable is the reasonable agreement of our reconstructed CO$_2$ with the stomata data between 15 and 20 Myrs BP (Fig. 6a). The stomata data capture a similar level of CO$_2$, but they were not included in the fit, as the temperature CO$_2$ slope is much

lower as indicated in Fig. 4. Note that around 10 Myr ago the B/Ca data indicate much lower CO_2 concentrations, in fact more in line with the GEOCARB (carbon-cycle model; Berner, 1994) estimates (Fig. 6a). Ultimately this implies an inconsistency between deep-sea benthic $\delta^{18}O$ reconstructions and B/Ca.

5 Long-term knowledge on climate sensitivity

Since we now have a continuous record of both temperature and CO_2, we can address the climate sensitivity in more detail. There are various ways to define climate sensitivity. Here we define climate sensitivity (S) as the functional dependency of changes in global surface temperature (ΔT_g) on CO_2, thus $\Delta T_g = f(CO_2)$. It is calculated from the radiative forcing (ΔR) caused by changes in CO_2, other greenhouse gases, and various fast and slow feedbacks (f). A general formulation for the global temperature is:

$$\Delta T_g = S \frac{\Delta R}{1 - f} \qquad (1)$$

In this general setting, changes in CO_2 might be the cause for climate change, thus represent the forcing term ΔR or a feedback, while the initial perturbation in the radiative balance might be caused by other processes. We will in the following develop a functional relationship between the global temperature and CO_2, in which we assume, that CO_2 is causing the radiative imbalance, thus $\Delta R = f(CO_2)$, which is then amplified by other processes. This by no means implies, that we believe that changes in CO_2 were always the driver for climate change over the last 20 Myr, but it is used to derive a functional relationship between ΔT_g and CO_2. The opposite procedure (forcing by other processes, and feedbacks by CO_2) is certainly a valid possibility. However, for reasons of simplicity we here follow only one of the two possible calculations.

From radiative transfer theory we know that due to the saturation of the absorption bands a logarithmic relationship has to be applied for the radiative forcing of CO_2:

$$\Delta R = \beta \ln \left(\frac{CO_2}{CO_{2,\text{ref}}} \right) \tag{2}$$

where ΔR is the radiative forcing in $W\,m^{-2}$, and β is estimated to be $5.35\,W\,m^{-2}$
5 (Myhre et al., 1998). This implies a radiative forcing of $-2.4\,W\,m^{-2}$ for the observed changes in CO_2 from LGM to present-day, and $+3.7\,W\,m^{-2}$ for a doubling of CO_2, with $CO_{2,\text{ref}} = 278\,ppmv$. Non-$CO_2$ greenhouse gases like CH_4 and N_2O enhance this direct radiative forcing of CO_2. For the last $800\,kyr$ this enhancement was about 30% (Köhler et al., 2010), which is approximated by a factor $\gamma = 1.3$.
10 The sensitivity S of the climate system to external forcing is typically described by the Charney sensitivity S_c (Charney et al., 1979), which includes the fast feedbacks of the system (water vapor, lapse rate, albedo, snow and sea ice, clouds). It is the quantity usually calculated by coupled ocean-atmosphere models. Here, we use a Charney sensitivity S_c derived from paleo data of $0.72\,K\,Wm^{-2}$ (Köhler et al., 2010). It is based
15 on a LGM cooling of $\Delta T_{g,\text{LGM}} = -5.8\,K$ (Schneider von Deimling et al., 2006), and a total radiative forcing $\Delta R_{\text{LGM}} = -9.5\,W\,m^{-2}$ (Köhler et al., 2010). This value for S_c takes into account that the LGM climate sensitivity is about 15% smaller than sensitivities calculated for future scenarios with $2 \times CO_2$, possibly caused by cloud microphysics (Hargreaves et al., 2007).
20 The total forcing of the system ($\Delta R'$) includes the forcing ΔR caused by all greenhouse gases, which is amplified by a feedback factor f consisting of the slow feedbacks not included in S_c. It represents the feedbacks from albedo changes caused by land ice, vegetation and dust.

$$\Delta R' = \frac{\gamma\,\Delta R}{1 - f} \tag{3}$$

25 A value for $f = 0.71$ is derived from proxy-based evidence (Köhler et al., 2010).

Full Screen / Esc

Printer-friendly Version

Interactive Discussion

In the previous section it was shown that we obtain a temperature change for the land masses in the NH, of 15 K for an ice age, about 2.5 times larger ($\alpha = 2.5$) than the global temperature change of slightly less than 6 K for LGM. Hence the final expression for the change of ΔT_{NH} can be written as:

$$\Delta T_{NH} \;=\; C \; \ln \frac{CO_2}{CO_{2,ref}} \tag{4}$$

with

$$C \;=\; \frac{\alpha \; \beta \; \lambda \; S_c}{1 - f} \tag{5}$$

Calculation of C ($\alpha = 2.5$, $\beta = 5.35$, $\gamma = 1.3$, $S_c = 0.72$, $f = 0.72$, $CO_{2,ref} = 278$) results in an indicative value of 43 K. Where it might be noted that application of $CO_{2,ref} = 278$ ppmv implies that ΔT_{NH} is expressed relative to pre-industrial levels.

The agreement between $C = 43$ K with the slope of the regression ($39 \pm 10\%$) derived from our modeled ΔT_{NH} and proxy CO_2 (Fig. 5) confirms that even with the limited data available we can argue that we have a reasonable understanding between temperature and CO_2 over the last 15 Myrs.

One of the major uncertainties here is probably the assumption that the ratio between the temperature change for the Northern Hemisphere and the global mean temperature is constant over time. Theories and observations on much warmer climate states suggest a decrease in the meridional temperature gradient implying a decrease in α. Hence, our result can be considered as the net effect of the decrease in α and the enhanced long-term feedbacks. The applied method does not allow separation of these effects, and therefore compensating variations in different mechanisms cannot be excluded. If α is much smaller for warmer climate conditions, it would imply that considerably higher CO_2 concentrations in the past are necessary to explain the benthic $\delta^{18}O$ record. Stomata, which are excluded from our fitting procedure, the GeoCarb data (Berner, 1994), and the B/Ca data do not indicate this.

449

Another source of uncertainty is the value for S_c. The value adopted here is derived from LGM conditions. Hargreaves et al., 2007 argue that this value is 15% larger than the value for $2 \times CO_2$. Our values for the Miocene maximum are close to those high CO_2 concentrations. A similar change in the sensitivity implies that C would decrease

5 to a value of 37 K, which is still within the range based on our modeled temperatures and the proxy CO_2 records. Here we keep C constant over time.

Too little information is available to attribute individual changes in the parameters over 20 Myrs. But given the fact that the fitted value of C based on the presented data in this paper, and the estimated value of C based on our knowledge of the system

10 (Köhler et al., 2010) are close to each other, implies that the combined effect of the key processes affecting benthic $\delta^{18}O$ records, temperature and CO_2 are incorporated sufficiently accurately for at least the period that there is ice on Earth. It also implies that the sensitivity of the climate in the past has been considerably different from the present-day climate. From the derived coefficients between temperature and CO_2 it

15 follows that for a 20 K cooling in ΔT_{NH} (or 8 K in T_g), the sensitivity was about 35% higher. This implies that care should be taken in the application of paleoclimate data for estimates of present-day changes.

6 Discussion and conclusion

Accepting the CO_2 concentration as presented in Fig. 1 with all its caveats, completes

20 the picture of the key climate variables over the last 20 Myrs. The figure shows a gradual decline from about 450 ppmv near 15 Myrs ago to a preindustrial level of 278 ppmv or a decrease of only 170 ppmv. This is about 1.7 times the increase in CO_2 concentration over the last century as well as 1.7 times the range in the ice-core record over the past 800 Kyrs. If we would have used only the ice-core record we would have ob-

25 tained Middle Miocene values, which are 300 ppmv above present-day level and the sensitivity would not agree with the analyses presented in the previous paragraph as

the sensitivity (C) would decrease to a value as low as 28.5 K. Hence the application of the inverse model and the stacked binning procedure is crucial for the results.

The question remains of course what causes these subtle changes in the carbon cycle on the long time scale. In order to answer this question much higher resolution and accuracy of CO_2 records are necessary. The large sensitivity implies that, in contrast to earlier conclusions (Hönisch et al., 2009), subtle changes in CO_2 (possibly internal), may have caused the MPT, when dominant 41-kyr glacial cycles evolved into a dominant 100-kyr rhythm (Van de Wal and Bintanja, 2009). Our results indicate an average change of only 23 ppmv between 1.5 Ma and 0.5 Ma, and also an increasing amplitude. This result seems to be more in line with a recent estimate by Lisiecki (2010) based on marine δ^{13}C measurements and the δ^{11}B data by Hönisch et al. (2009) than with the B/Ca derived CO_2 data by Tripati (2009), which indicates a larger change in CO_2. However, the trend in CO_2 over time is too small given the accuracy of the applied methods to draw firm conclusions on this point.

With respect to the inception of the Northern Hemisphere ice around 2.7 Myrs ago our results indicate that the trend in CO_2 before the inception is strong (see Fig. 1d), and that the inception takes place once the long-term average concentration drops below 265 ± 20 ppmv (Fig. 6b). So for this climate transition a change in CO_2 seems to be more important than for the mid-Pleistocene transition.

More importantly, the self-consistency of our approach should enable researchers from various disciplines to identify more easily, how the various CO_2 proxies can be understood in the broader framework of long-term climate change.

Various geological processes important during the last 20 Myr such as mountain uplift (e.g. Foster et al., 2010) and changes in the gateways are not considered here. However, for global climate changes CO_2 induced changes dominate as shown by Henrot et al. (2010), who argued based on a model of intermediate complexity that geological processes like mountain building and changes in ocean gateways are of secondary importance for global temperature and can not explain the proxy reconstructions of the change in temperature within their modeling framework.

Title Page

Abstract · Introduction

Conclusions · References

Tables · Figures

|◄ · ►|

◄ · ►

Back · Close

Full Screen / Esc

Printer-friendly Version

Interactive Discussion

As final remark we stress that the changing sensitivity implies that care should be taken to use paleo data as analogue for present-day conditions. This is not to disqualify paleo climate research in general, but rather a warning. Paleo data provide the range of natural fluctuations, but the rate of change of key variables is shown to be depending on the state of the system (Köhler et al., 2010), the time scale of interest and the processes at stake, which are not necessarily similar in the past as for present-day climate change.

References

Barker, S., Diz, P., Vantravers, M. J., Pike, J., Knorr, G., Hall, I. R., and Broecker, W. S.: Interhemispheric Atlantic seesaw response during the last deglaciation, Nature, 457, 1007–1102, 2010.

Berner, R. A.: GEOCARB II: A revised model of atmospheric CO$_2$ over Phanerozoic time, Am. J. Sci., 294, 56–91, 1994.

Bintanja, R. and van de Wal, R. S. W.: North American ice-sheet dynamics and the onset of 100,000-year glacial cycles, Nature, 454, 869–872, 2008.

Bintanja, R., van de Wal, R. S. W. and Oerlemans, J.: A new method to estimate ice age temperatures, Clim. Dynam., 24(2–3), 197–211, 2005a.

Bintanja, R., van de Wal, R. S. W. and Oerlemans, J.: Modelled atmospheric temperatures and global sea levels over the past million years, Nature, 437, 125–128, doi:10.1038/nature03975, 2005b.

Charney, J. G., Arakawa, A., Baker, D. J., Bolin, B., Dickinson, R. E., Goody, R. M., Leith, C. E., Stommel, H. M., and Wunsch, C. I.: Carbon Dioxide and Climate: A Scientific Assessment, Natl. Acad. Sci., 33 pp., 1979.

Clark, P. U., Alley, R. B., and Pollard, D.: The middle Pleistocene transition: Characteristics, mechanisms, and implication for long-term changes in atmospheric pCO$_2$, Quaternary Sci. Rev., 25, 3150–3184, 2006.

Title Page

Abstract | Introduction

Conclusions | References

Tables | Figures

◄ | ►

◄ | ►

Back | Close

Full Screen / Esc

Printer-friendly Version

Interactive Discussion

De Boer, B., van de Wal, R. S. W., Bintanja, R., Lourens, L. J., and Tuenter, E.: Cenozoic global ice-volume and temperature simulations with 1-D ice-sheet models forced by benthic $\delta^{18}O$ records, Ann. Glaciol., 51(55), 23–33, 2010.

Foster, G. L., Lunt, D. J., and Parrish, R. R.: Mountain uplift and the glaciation of North America - a sensitivity study, Clim. Past, 6, 707–717, doi:10.5194/cp-6-707-2010, 2010.

Hargreaves, J. C., Abe-Ouchi, A., and Annan, J. D.: Linking glacial and future climates through an ensemble of GCM simulations, Clim. Past, 3, 77–87, doi:10.5194/cp-3-77-2007, 2007.

Hays, J. D., Imbrie, J., and Shackleton, N. J.: Variations in the Earth's orbit: Pacemaker of the ice ages, Science, 194, 1121–1132, 1976.

Henrot, A.-J., François, L., Favre, E., Butzin, M., Ouberdous, M., and Munhoven, G.: Effects of CO_2, continental distribution, topography and vegetation c hanges on the climate at the Middle Miocene: a model study, Clim. Past, 6, 675–694, doi:10.5194/cp-6-675-2010, 2010.

Hönisch, B., Hemming, N. G., Archer, D., Siddall, M., and McManus, J. F.: Atmospheric carbon dioxide concentration across the mid-Pleistocene transition, Science, 324, 1551–1553, 2009.

Huybers, P.: Glacial variability over the last two million years: An extended depth-derived age model, continuous obliquity pacing, and the Pleistocene progression, Quaternary Sci. Rev. 26, 37–55, 2007.

Imbrie, J. and Imbrie, J. Z.: Modelling the climatic response to orbital variations, Science, 207, 942–953, 1980.

Jansen, E. J., Overpeck, J., Briffa, K. R., Duplessey, J.-C., Joos, F., Masson-Delmotte, V., Olago, D., Otto-Bliesner, B., Peltier, W. R., Rahmstorf, S., Ramesh, R., Raynaud, D., Rind, D., Solomina, O., Villalba, R., and Zhang, D.: Paleoclimate, in: Climate change 2007: The physical Science basis. Contribution of Working Group I to the Fourth Assessment Report of the Intergovernmental Panel on Climate Change, 433–497, 2007.

Köhler, P. and Bintanja, R.: The carbon cycle during the Mid Pleistocene Transition: the Southern Ocean Decoupling Hypothesis, Clim. Past, 4, 311–332, doi:10.5194/cp-4-311-2008, 2008.

Köhler, P., Bintanja, R., Fischer, H., Joos, F., Knutti, R., Lohmann, G., and Masson-Delmotte, V.: What caused Earth's temperature variations during the last 800,000 years? Data-based evidence on radiative forcing and constraints on climate sensitivity, Quaternary Sci. Rev., 29, 129–145, 2010.

Title Page

Abstract | Introduction

Conclusions | References

Tables | Figures

|◄ | ►|

◄ | ►

Back | Close

Full Screen / Esc

Printer-friendly Version

Interactive Discussion

Kürschner, W. M., Kvacek, Z., and Dilcher, D. L.: The impact of Miocene atmospheric carbon dioxide fluctuations on climate and the evolution of terrestrial ecosystems, P. Natl. Acad. Sci., 105(2), 449–453, 2008.

Lambeck, K. and Chapell, J.: Sea level change through the last glacial cycle, Science, 292(5517), 679–686, 2001.

Lear, C. H., Elderfield, H., and Wilson, P. A.: Cenozoic deep-sea temperatures and global ice volumes from Mg/Ca in benthic formaniferal calcite, Science, 287(5451), 269–272, 2000.

Lisiecki, L. E.: A benthic δ^{13}C-based proxy for atmospheric PCO_2 over the last 1.5 Myr, Geophys. Res. Lett., 37, L21708, doi:10.1029/2010GL045109, 2010.

Lüthi, D., Floch, M., Le Bereiter, B., Blunier, T., Barnola, J.-M., Siegenthaler, U., Raynaud, D., Jouzel, J., Fischer, H., Kawamura, K., and Stocker, T. F.: High-resolution carbon dioxide concentration record 650,000–800,000 years before present, Nature, 453, 379–382, 2008.

Milankovitch, M.: Kanon der Erdbestrahlung und seine Anwendung auf das Eiszeitenproblem, Special Publications, Royal Serbian Acadademy, 132, 1941.

Miller, K. G., Kominz, M. A., Browning, J. V., Wright, J. D., Mountain, G. S., Katz, M. E., Sugarman, P. J., Cramer, B. S., Christie-Blick, N., and Pekar, S. F.: The Phanerozoic record of global sea level change, Science, 310(5752), 1293–1298, 2005.

Müller, R. D., Sdrolias, M., Gaine, C., Steinberger, B., and Heine, C.: Log-term sea-level fluctuations driven by ocean basin dynamics, Science, 319, 1357–1362, 2008.

Myhre, G., Highwood, E. J., Shine, K. P., and Stordal, F.: New estimates of radiative forcing due to well mixed greenhouse gases, Geophys. Res. Lett., 25, 2715–2718, 1998.

Pagani, M., Zachos, J. C., Freeman, K., Tipple, B., and Bohaty, S.: Marked decline in atmospheric carbon dioxide concentrations during the Paleogene, Science, 309(5734), 600–603, 2005.

Pagani, M., Liu, Z., LaRiviere, J., and Ravelo, A.: High Earth-system climate snsitivity determined from Pliocene carbon dioxide concentrations, Nat. Geosci., 3, 27–30, 2009.

Pearson, P. N. and Palmer, M. R.: Atmospheric carbon dioxide concentrations over the past 60 million years, Nature, 406, 695–699, 2000.

Petit, J. R., Jouzel, J., Raynaud, D., Barkov, N. I., Barnola, J.-M., Basile, I., Bender, M., Chapellaz, J., Davis, M., Delaygue, G., Delmotte, M., Kotlyakov, V. M., Legrand, M., Lipenkov, V. Y., Lorius, C., Pépin, L., Ritz, C., Saltzmann, E., and Stievenard, M.: Climate and atmospheric history of the past 420 000 years from the Vostok ice core, Antarctica, Nature, 399, 429–436, 1999.

Title Page

Abstract | Introduction

Conclusions | References

Tables | Figures

|◄ | ►|

◄ | ►

Back | Close

Full Screen / Esc

Printer-friendly Version

Interactive Discussion

Raymo, M. E.: The initiation of Northern Hemisphere glaciation, Annu. Rev. Earth Planet. Sci. 22, 353–383, 1994.

Rohling, E. J., Grant, K., Bolshaw, M., Roberts, A. P., Siddall, M., Hemleben, Ch., and Kucera, M.: Antarctic temperature and global sea level closely coupled over the past five glacial cycles, Nat. Geosci., 2(7), 500–504, 2009.

Ruddiman, W. F.: A paleoclimatic Enigma?, Science, 328(5980), 838–839, doi:10.1126/science.1188292, 2010.

Ruddiman, W. F.: Earth's climate, W. H. Freeman and Company, New York, 2001.

Ruddiman, W. F.: Orbital insolation, ice volume and greenhouse gases, Quaterny Sci. Rev., 22, 1597–1629, 2003.

Schneider von Deimling, T., Ganopolski, A., Held, H., and Rahmstorf, S.: How cold was the Last Glacial Maximum?, Geophys. Res. Lett., 33, L14709, doi:10.1029/2006GL026484, 2006.

Seki, O., Foster, G. L., Schmidt, D. N., Mackensen, A., Kawamura, K., and Pancost, R. D.: Alkenone and boron-based Pliocene pCO_2 records, Earth Planet. Sc. Lett., 292, 201–211, 2010.

Siegenthaler, U., Stocker, T. F., Monnin, E., Lüthi, D., Schwander, J., Stauffer, B., Raynaud, D., Barnola, J., Fischer, H., Masson-Delmotte, V., and Jouzel, J.: Stable carbon cycle-climate relationship during the Late Pleistocene, Science, 310, 1313–1317, 2005.

Tripati, A. K., Roberts, C. D., and Eagle, R. A.: Coupling of CO_2 and ice sheet stability over major climate transitions of the last 20 million years, Science, 326, 1394–1397, 2009.

Tziperman, E. and Gildor, H.: On the mid-Pleistocene to 100-kyr glacial cycles and the asymmetry between glaciation and deglaciation times, Paleooceanography, 18, 1001, 2003.

Van de Wal, R. S. W. and Bintanja, R.: Changes in temperature, ice and CO_2 during the Mid-Pleistocene Transition, Science, E Letter, 18 September, 2009.

Zachos, J. C., Dickens, G. R., and Zeebe, R. E.: An early Cenozoic perspective on greenhouse warming and carbon-cycle dynamics, Nature, 451, 279–283, 2008.

Zeebe, R. E. and Wolf-Gladrow, D. A.: CO_2 in Seawater: Equilibrium, Kinetics, Isotopes, Elsevier Science Publishing, Elsevier Oceanography Book Series, 65, 346 pp., 2001.
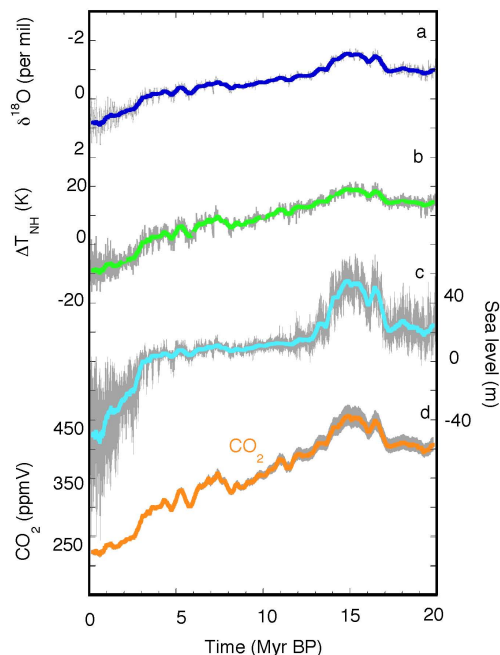
Title Page

Abstract | Introduction

Conclusions | References

Tables | Figures

Back | Close

Full Screen / Esc

Printer-friendly Version

Interactive Discussion

Fig. 1. Records of key climate variables over the last 20 Myrs. Forcing of the model is the stacked benthic $\delta^{18}O$ record **(a)**, dark blue, Zachos et al., 2008. Output is a consistent record for the Northern Hemisphere temperature change **(b)**, green – and sea level **(c)**, light blue. The reconstructed CO_2 record **(d)**, orange – is obtained by inverting the relation between NH temperatures and CO_2 data **(d)**. Here it is shown as 400-kyr running mean. Data used for the reconstruction are indicated with different colours – see caption Fig. 3 for the details **(d)**. The $\delta^{18}O$ curve is smoothed in order to clarify the gradual decrease over time. All data are available every 0.1 kyr. The thick lines represent 400-kyr running mean. Gray error bars indicate the standard deviation of model input and output. For CO_2 the error bar is calculated as 400-kyr running mean, for the other records it is the standard deviation on the 0.1 kyr value as used in the model.

Back | Close

Full Screen / Esc

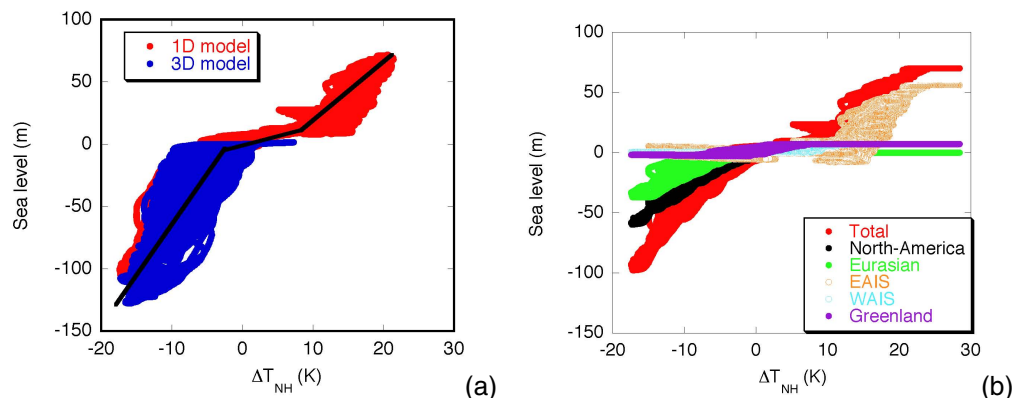Printer-friendly Version

Interactive Discussion

Fig. 2. (a) Sea-level change is shown as a function of the reconstructed temperature for a set of 3-D NH ice sheets (blue) and for a set of five 1-D ice-sheet models (red) (Bintanja and Van de Wal, 2008; De Boer et al., 2010). The more sophisticated 3-D results are validated by observation of sea level (Lambeck and Chapell, 2001; Rohling et al., 2009). The 1-D results are in line for the colder climate condition with the 3-D results. The warm temperatures in combination with the sea-level change resemble the melt of SH ice. The thick lines in the lower panel show the mean trends, emphasizing the low gradient for the present-day climate centred around zero. **(b)** The response of the individual ice sheets. Note the strong transient and non-linear response for each ice sheet.
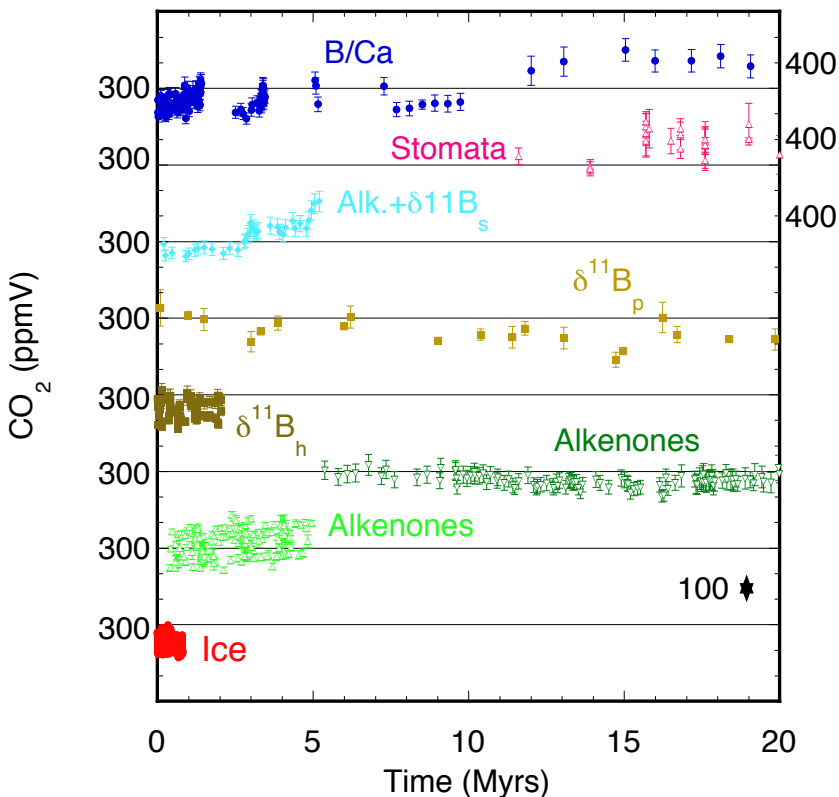
Fig. 3. CO_2 records as a function of time, indicating the inhomogeneous distribution in amount and range for the different proxies. Data are ordered randomly from top to bottom being B/Ca (Tripati et al., 2009), stomata data (Kürschner et al., 2008), alkenones combined with $\delta^{11}B_s$ (Seki et al., 2010), $\delta^{11}B_p$ (Pearson and Palmer, 2000), $\delta^{11}B_h$ (Hönisch et al., 2009), alkenones (Pagani et al., 2005, 2010) and ice (Petit et al., 1999; Siegenthaler et al., 2005; Lüthi et al., 2008). Minor ticks for the CO_2 concentrations are every 100 ppm for all records. The symbols and colors for the different proxies are similar in all figures.

Title Page

Abstract | Introduction

Conclusions | References

Tables | Figures

|◄ | ►|

◄ | ►

Back | Close

Full Screen / Esc
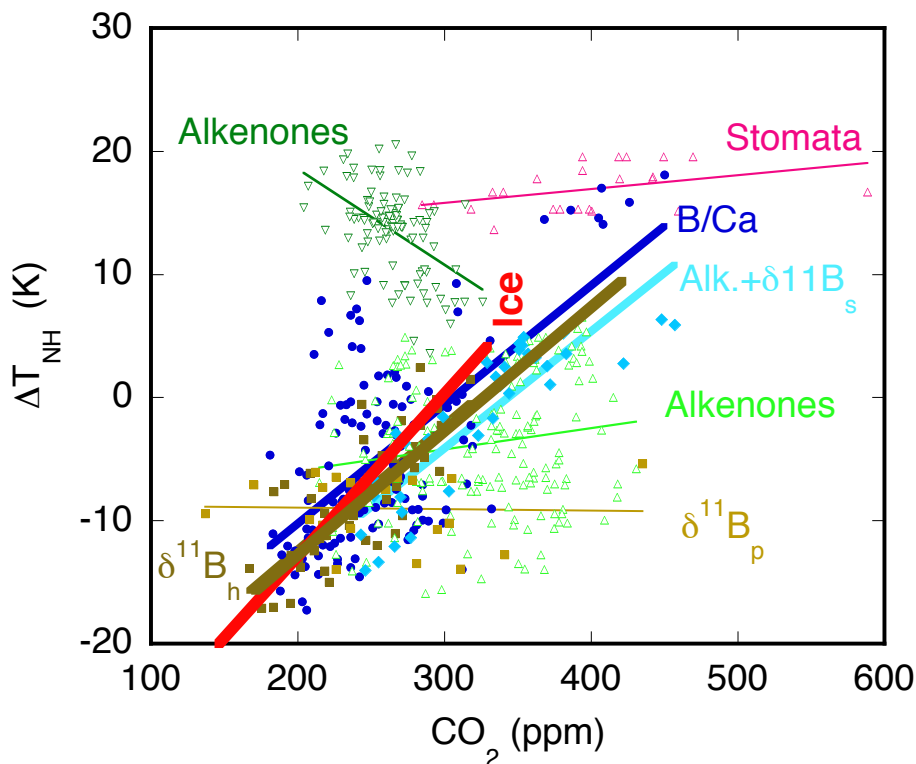
Printer-friendly Version

Interactive Discussion

Fig. 4. Scatter plot of the different CO_2 proxies as a function of the reconstructed temperature, which is derived from, the benthic $\delta^{18}O$ record as shown in Fig. 1. Only records with filled symbols $\delta^{11}B_h$ (Hönisch et al., 2009), B/Ca (Tripati et al., 2009), alkenones + $\delta^{11}B_s$ (Seki et al., 2010) and the ice-core record (Petit et al., 1999; Siegenthaler et al., 2005; Lüthi et al., 2008) are used to calculate the climate sensitivity, $C = 39$ K. For reasons of transparency CO_2 is plotted in ppmv. If CO_2 would be plotted as $\ln(CO_2/CO_{2,ref})$ a similar picture emerges. The latter is physically more consistent as it takes the saturation of the absorption bands into account.
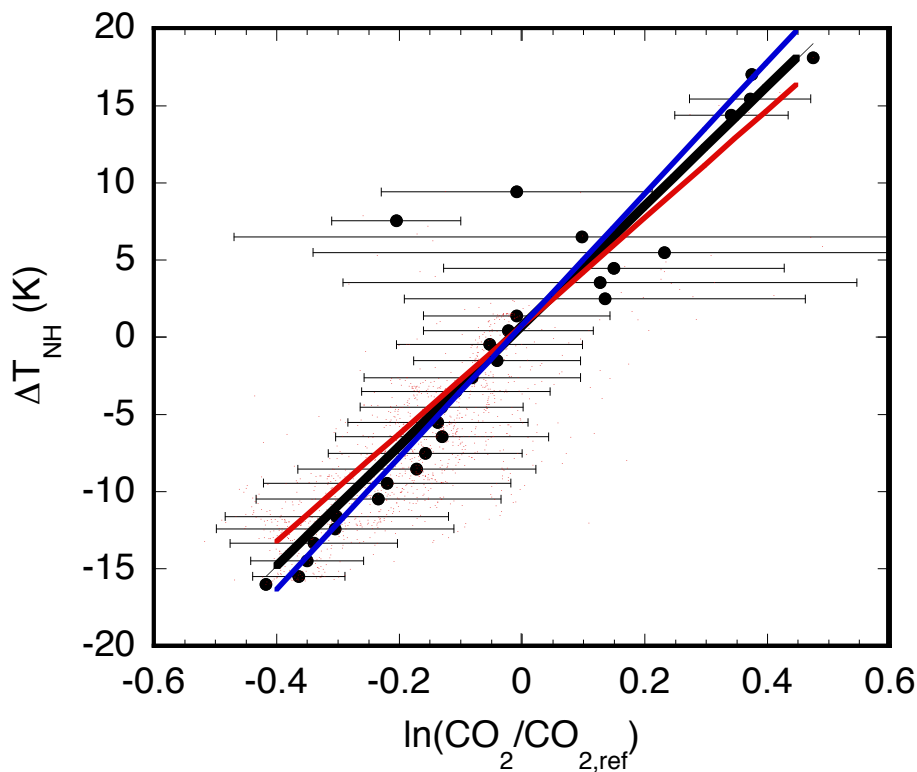
Title Page

Abstract | Introduction

Conclusions | References

Tables | Figures

|◄ | ►|

◄ | ►

Back | Close

Full Screen / Esc

Printer-friendly Version

Interactive Discussion

Title Page

Abstract | Introduction

Conclusions | References

Tables | Figures

|◄ | ►|

◄ | ►

Back | Close

Full Screen / Esc

Printer-friendly Version

Interactive Discussion

Fig. 5. The selected (n = 1287) proxy CO$_2$ data (red dots) binned in intervals of 1 K NH temperature change. The error bars represent one standard deviation variability of the data in the selected temperature interval. The additional lines show the range in C values from different weighing tests, blue C +10%, red C −10%.
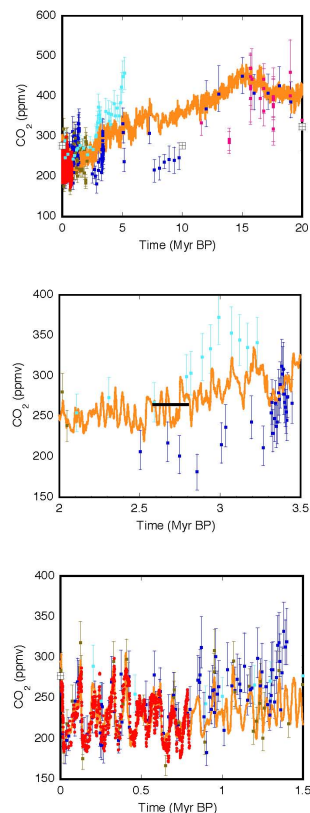
Fig. 6. Comparison of reconstructed CO$_2$ record with $C = 39$ K, with proxy records (symbols as in Fig. 3). Panel **(a)** for the full 20 Myr period, **(b)** for the period around the NH hemisphere inception and **(c)** for the mid-Pleistocene transition. Note that the vertical scale is different for the different panels. The horizontal bar in panel **(b)** indicates the onset of major glaciation in the Northern Hemisphere.